UNSTEADY PHENOMENA DURING OPERATION OF THE SSME FUEL FLOWMETER

Bogdan Marcu
Boeing
Rocketdyne Propulsion & Power
6633 Canoga Ave
Canoga Park, CA 91309-7922

ABSTRACT

This report describes a part of the analysis carried in support of the SSME Fuel Flowmeter redesign, addressing an intensely researched phenomenon known as "shifting" of the flowmeter constant value. It consists of a sudden change in the flowmeter indication, which occurs simultaneously with the onset of an oscillatory variation of the rotor speed. The change in the flowmeter indications does not correspond to a real change in the volumetric flow through the device. Several causes have been investigated in detail, in the past, without conclusive evidence towards a cause of this phenomenon. The present analysis addresses the flow physics through the flowmeter by assembling results from 3-D CFD calculations, airfoil C_D/C_L performance curves and mass moment of inertia characteristics of the rotor into a synergistic calculation which simulates the unsteady regime of the flowmeter operation. The results show that the 4-bladed rotor interacts with the periodic flow pattern created behind the flow straightener upstream in a manner that generates a steady, periodic fluctuation in the rotor's speed. The amplitude of this fluctuation is significantly smaller than the 0.5% of mean speed threshold which constitutes a flight operational limit. When manufacturing errors occur, however, the fluctuations are amplified and can generate a significant apparent change in the flowmeter indication. Two types of possible fabrication errors—which can occur even for parts fabricated within the accepted tolerances for the blade airfoil—are presented, together with their effect on the flowmeter operation.

NOMENCLATURE

U	blade tangential velocity
Ca	fluid axial velocity
W	fluid relative velocity
ρ	fluid density
α	blade stagger angle
β	angle of relative fluid velocity
i	flow incidence angle on the blade
θ	blade angular position
C_D, C_L	drag and lift coefficients
ρ	fluid density
b	blade chord length
K_f	flow meter calibration constant for engine operation
K_{fw}	flow meter calibration constant determined from water flow test

1. INTRODUCTION

The Space Shuttle Main Engine uses a turbine type flow meter [6] to control the amount of fuel delivered to the engine and the mixture ratio between the fuel and oxidizer. The flow meter is located in a duct between the low pressure fuel pump discharge and the high pressure fuel pump inlet. The meter translates the volume flow of the liquid hydrogen based on its rotor speed and a calibration constant, denominated as K_f, which relates the fuel volume flow rate to the rotor's rotational speed though a proportionality relationship $K_f = 4\ RPM/GPM$, where ***RPM*** is the rotor speed in rotations per minute and ***GPM*** the fuel volumetric flow rate in gallons per minute.

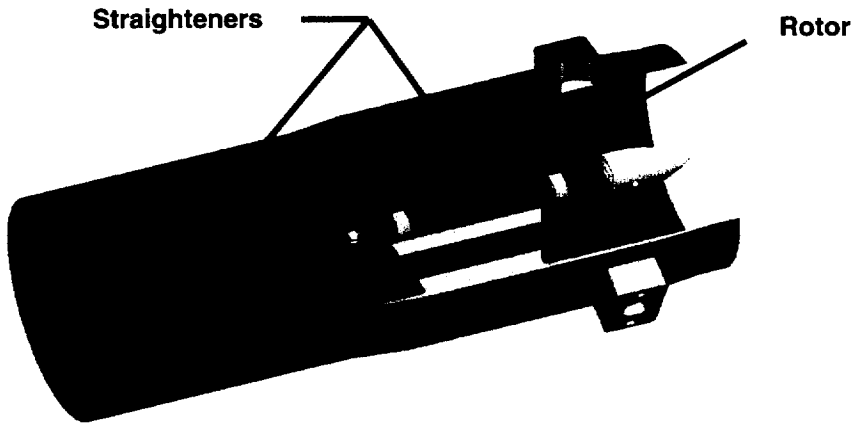

Figure 1. SSME Fuel Flometer Configuration

The flowmeter—shown in figure 1—consists of a set of honeycomb flow straighteners, followed by a 4-blade turbine rotor whose speed of rotation is picked up by a magnetic sensor.

Over the years of the Space Shuttle Main Engine (SSME) operation, a certain behavior was observed in the flow-meter operation [1, 2]. At certain regimes, an apparent shift seems to occur in the K_f value, without a real change in the fuel volume flow rate. The K_f shift phenomenon also appears to be associated with a fluctuation in the rotor's speed. A typical example of such behavior is shown in figure 2. The detailed plot of the onset of the anomalous behavior shows that, while the real volume flow (denoted as facility flow) decreases slightly, the flowmeter indicates a slight increase. Sometimes it is apparent that the onset of such behavior is associated with significant fluctuations in the flowmeter speed, as shown in figure 3. Such fluctuations may be of high frequency, but since the rotation is only sampled 4 times per one complete revolution, aliasing occurs in the measurements. Hence, the term of "aliasing" has been associated with the rotor speed fluctuations, occurring simultaneously with the K_f shifting.

Extensive work has been done to investigate the phenomenon. The effects of engine vibrations on the duct flow have been assessed [2]. Also, a different analysis [3] has demonstrated a rotor sensitivity to the flow turbulence intensity. No conclusive evidence was found that either condition is the cause of the shifting. Recently, an unsteady 2-D CFD analysis by A. Hadid [5], and a pseudo-unsteady 3-D CFD analysis by E. Ascoli et.al. [4] have found that when the blade passes the strong wakes in the flow pattern generated behind the hex flow straightener, there are momentary stall-like flow regimes on the blade, which slow down the rotor. Both authors suggests that the occurrence of successive stalls may produce effects similar the K_f shifting phenomenon, associated with a high frequency oscillation in the rotor.

The present analysis addresses the problem in its entire physics, i.e. the coupling of the flow field distortions with the blade aerodynamics and the rotor's dynamics, in an effort towards explaining the underlying nature of the K_f shifting phenomenon.

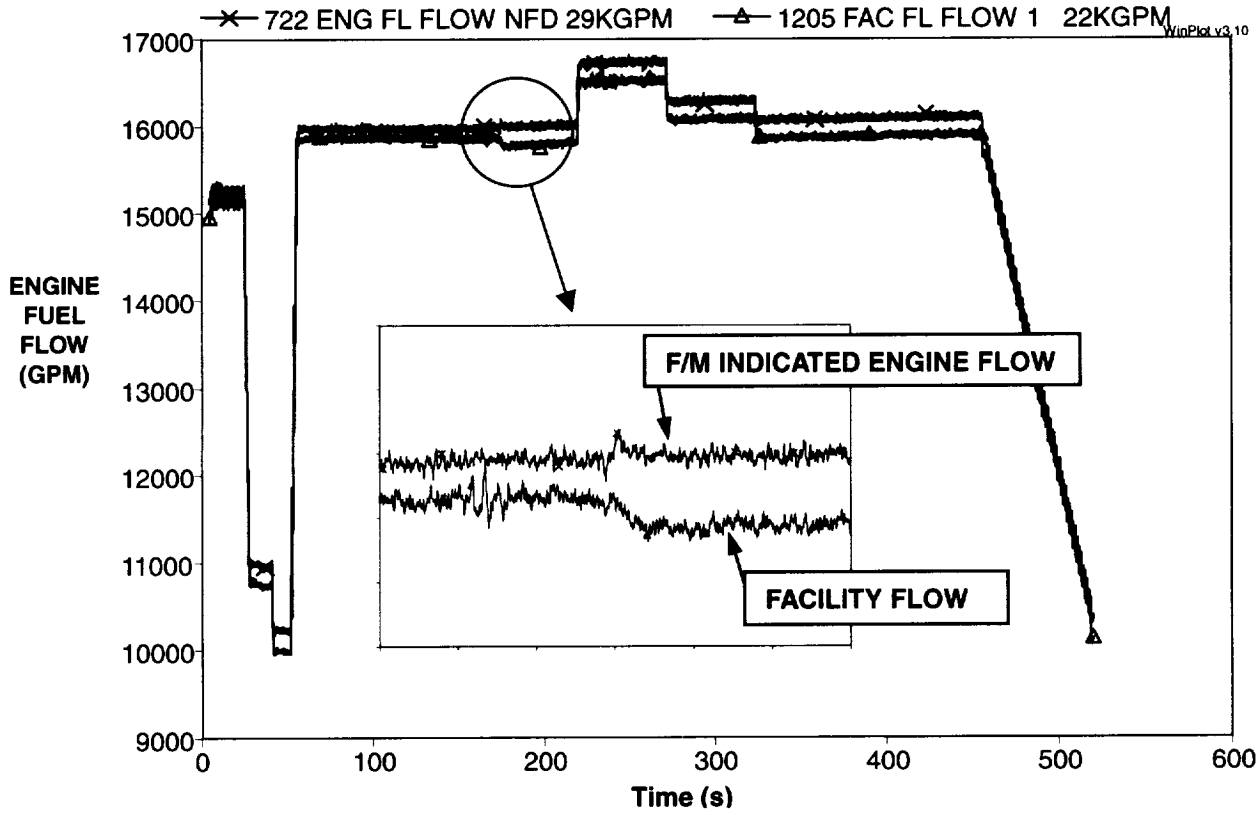

Figure 2. An example of an apparent shift of the flowmeter's indication. While the volume flow actually decreases slightly—as shown by the ground test facility flow measurement—the flowmeter indication increases slightly. Since the meter indication is derived from it's speed measurement, it turns out that the meter's rotor rotates faster than it should (i.e. faster than it did when it was calibrated). In most other instances, it appears to be rotating slower. Such a situation is equivalent to a change in the proportionality constant K_f which relates the rotor speed to the volume flow, hence the expression "K_f shifting"..

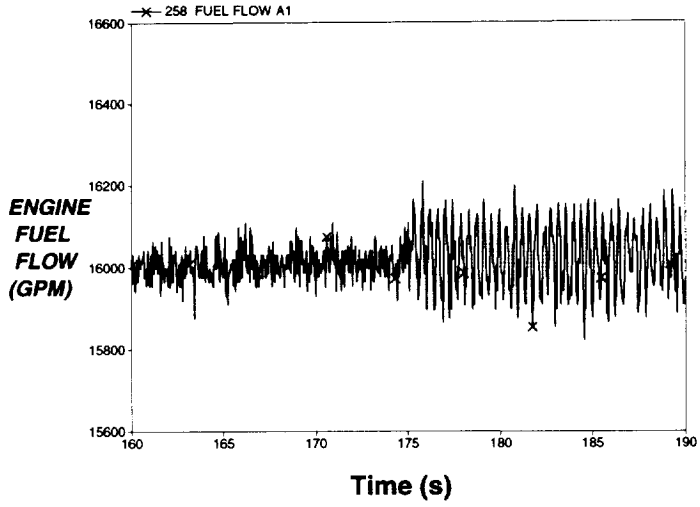

Figure 3. In most of the cases of K_f shifting, the onset of the K_f apparent value shift is associated with significant oscillations in the flowmeter's reading.

2. THE FLOWMETER MODEL

In order to organize a fluid dynamics model for the flowmeter, one must understand a significant difference between a typical turbine destined to produce power, and the turbine flowmeter rotor at hand. A typical turbine rotor operates by organizing the working fluid flow within the channel formed between two adjacent blades in a way that maximizes blade loading and allows a high degree of turning of the fluid, thus producing a significant torque. The flowmeter rotor on the other hand (shown in figure 4), uses only 4 blades that operate practically independent of each other—in the sense that one cannot speak of a channel flow in between these blades—as isolated rotating airfoils. If the rotor were to operate in a smooth, uniform incoming flow, its blades should operate at very small incidence angles at every radius. The situation is depicted in figure 5. The incoming flow has a uniform axial velocity C_a while the rotor blade has the tangential velocity U as shown. Adding the two vector velocities results in the relative velocity with respect to the blade, W. The blade stagger angle α is not quite aligned with the relative velocity angle β, as the relative velocity impinges on the blade's leading edge at a small incidence angle i. Since the blade profile is symmetric, the small incidence angle is necessary to produce some lift, besides drag. Only the tangential components of the forces acting on the rotor blade are of interest here. The blade will adjust its tangential velocity in a way that will produce a very small incidence angle i for which the tangential component of the drag force and rotor miscellaneous friction resistances R_f will be compensated by the tangential component of lift. Due to the free-vortex blade twist $\alpha = \alpha(R)$ (figure 5b), this situation occurs at every radius R of the blade.

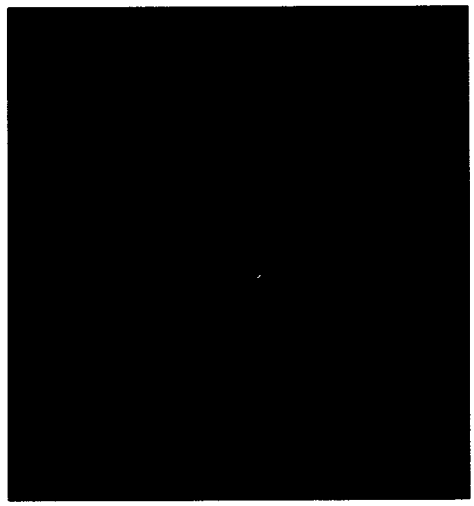

Figure 4. The flow meter rotor.

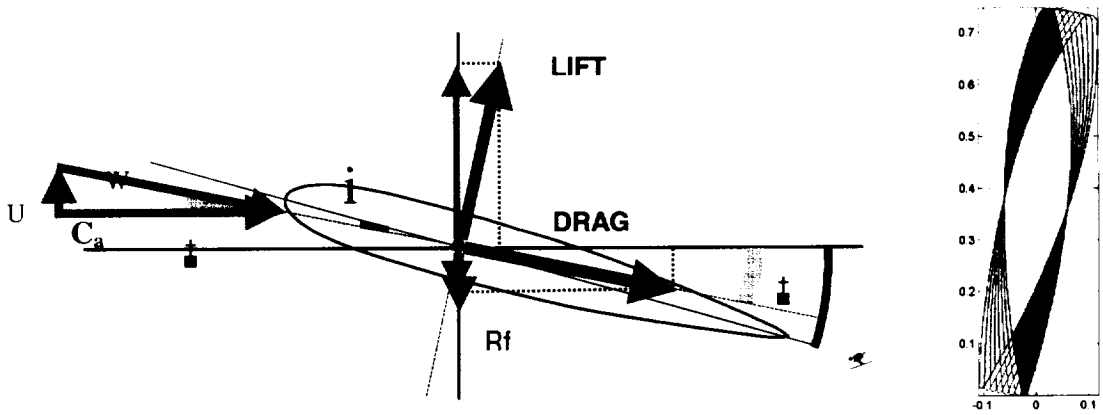

Figure 5. a) The blade load and force decomposition on the rotor blade b) The blade radial twist

However, the incoming flow is not uniform. The hexagonal channels of the straightener generate a flow pattern as shown in figure 6. The pattern is periodic in the tangential direction, characterized by a 12N and 18 N periodicity in the axial fluid velocity, therefore, in the model shown in figure 5 the axial fluid velocity becomes a forcing function $Ca = Ca(t)$, since the rotor will "feel" an unsteady incoming fluid axial velocity as it passes through the wakes existent in the flow pattern behind the flow straightener. If the rotor has a mass moment of inertia I, at every moment it's motion is governed by the dynamic equation of motion

$$I\frac{d^2\theta(t)}{dt^2} = T[\theta(t),\alpha(R),C(R,\alpha,\theta(t))] \qquad (1.)$$

where $\theta = \theta(t)$ is the rotor's angular position, t is the time, and T is the torque produced by the resultant force on the blade according the model in figure 5, i.e. $T = T[\theta(t), \alpha(R), Ca(R, \alpha, \theta(t))]$. The torque expression in (1.) is a complicated relationship due to the simultaneous nonlinear two-way coupling between the rotor position and the aerodynamic forces on the blade. In order to solve for the dynamic equation of motion, one must rely on numerical procedures. A numerical model has been assembled as follows.

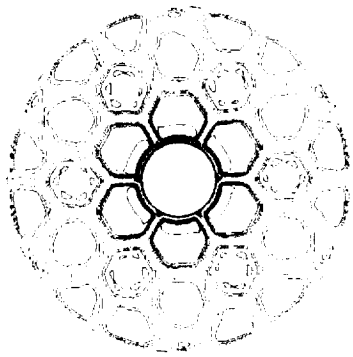

Figure 6. Axial fluid velocity field intensity pattern (from CFD calculations) behind the flow straightener

The flow field behind the flow straightener $Ca(R, \alpha, \theta)$ has been generated by a 3-D CFD calculation in reference [4]. One can assume that the coupling between the flow field and the rotor motion is strong in the direction flowfield→rotor motion and very weak in the reverse direction rotor motion→flowfield, or otherwise stated, the presence of the rotor does not influence the flow pattern since the rotor has only 4 blades (very small blockage) and carries no load, while the flow is extremely energetic during the SSME operation. Relying on a numerically known incoming flowfield, the instantaneous value of the blade torque T can be computed by an integration along the radius of the local torque produced at each radial location (in fact a narrow bin) by the aerodynamic forces described in figure 5 (see also figure 7).

$$T(t) = \int_{r_{hub}}^{r_{tip}} dT \qquad (2.)$$

$$dT = dF_T R \qquad (3.)$$

$$dF_T = \frac{1}{2}\rho \cdot b \cdot W^2(R) \times \qquad (4.)$$

$$[C_L(R)\cdot\cos(\beta(R)) - \zeta \cdot C_D(R)\cdot\sin(\beta(R))]\cdot dR$$

where ζ is an empirical parameter allowing for the calibration of the numerical model with experimental data. Equation (1) is integrated numerically using a 4th order Runge-Kutta scheme, considering each of the 4 blades simultaneously, clocked at 90 degrees from each other. The C_D and C_L performance is modeled from NACA 4 digit series airfoils. The airfoil of each blade is divided in 32 radial bins for which the Drag and Lift forces are calculated at each time step based on C_D/C_L modeling, incidence i and incoming relative flow velocity W. The numbers are then integrated according to expressions (2) through (5).

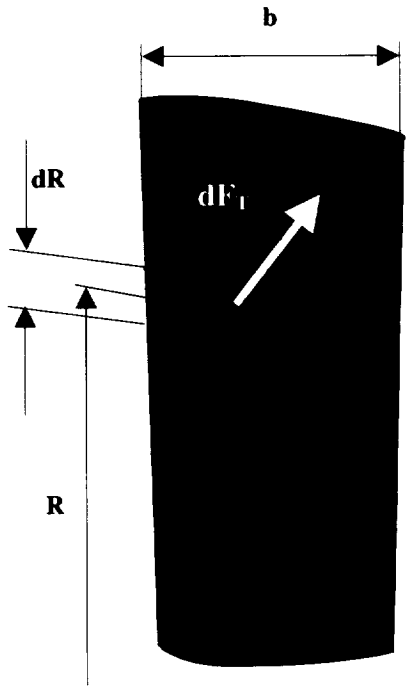

Figure 7. Force/Torque integration on a rotor blade.

3. ANALYSIS

3.1 Quasi-steady regime

The numerical procedure presented in the previous section has been applied for the computation of the rotor response time to a sudden change in the flow rate. The results are presented in Figure 8 for two flowmeter configurations using the orginial SSME flowmeter rotor with ***I=0.0035*** lbm ft^2, and a redesigned rotor with ***I=0.0039*** lbm ft^2 [7]. The simulation results confirm the measured response time, which is of the order of 6 milliseconds for both rotors.

One important detail can be observed in figure 8a. After the rotor responds to a change in the volumetric flow rate, it operates at a quasi-steady regime characterized by a stable and periodic fluctuation in speed, with very small amplitude. The amplitude of the fluctuations shown is 0.28% and 0.21% of the mean speed value for the original and the new design respectively. Figure 8b show the fluctuating component of the rotor speed for the original rotor, calculated at 115% engine Rated Power Level (RPL). The spectral analysis of the fluctuation is shown in figure 8c. The dominant frequency (791 Hz) corresponds to the 12N symmetry of the hexagonal flow straightener pattern.

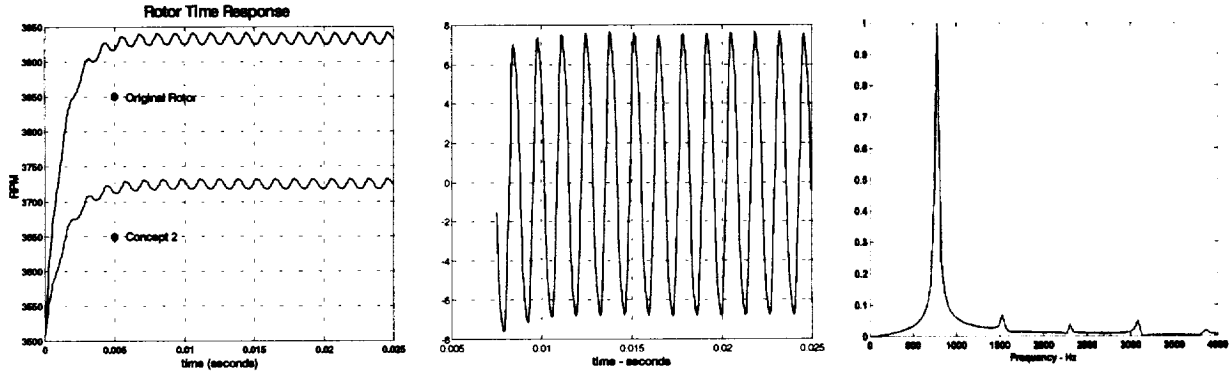

(a) *(b)* *(c)*

Figure 8. a) Rotor time response to a change in flow volumetric rate. b) Rotor speed fluctuation componend during quasi-steady operation. c) spectral analysis of the fluctuating component: the peak corresponds to 12N frequency.

3.2 Possible manufacturing errors and their effects

The shifting and speed oscillation occurrences during the flowmeter operations have been, in several cases, well correlated with "off-print" rotor parts. Specifically, the blade airfoil had been manufactured outside the tolerance field. This correlation has led to a careful assessment of the possible type of errors which can occur, and their effect on then rotor operation [7]. In the following, a classification of the airfoil errors is presented from the point of view of their aerodynamic effect.

One type of a manufacturing error is one during which the blade airfoil at a certain radius is twisted, or rotated, within the accepted tolerance field. The situation is shown in figure 9. All points on the fabricated blade are within tolerance, yet, by a biased distribution of differences from print, the profile has an extra twist, which adds to the design blade stagger angle α as an alteration ε. A tolerance band of ± 0.003 inches will allow for a maximum of $\pm 0.556^{\circ}$

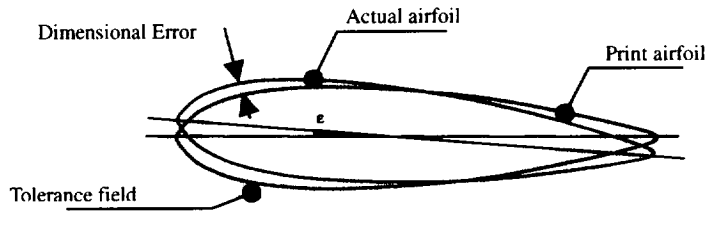

Figure 9. Manufacturing error of Type I, altering the blade stagger angle by a fraction ε.

deviation from the intended blade stagger angle. For a case of ±0.010 inches tolerance band, the deviation from the intended blade stagger angle can be as large as ±2.0°.

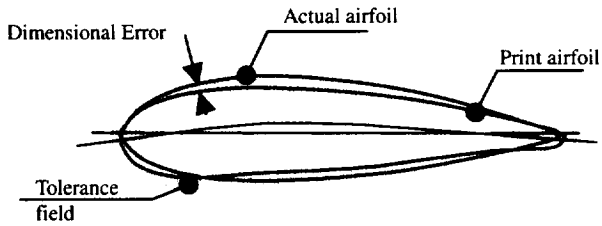

Figure 10. Manufacturing error of Type II, altering the blade mean line camber.

Another type of manufacturing error is one that disturbs the symmetry of the blade. The deviations from the blade profile print, while within the accepted tolerance band, group as shown in figure 10, distorting the geometry of the profile from a symmetric profile to an asymmetric one with a cambered mean line. Such a distortion changes the airfoil lift and drag characteristics. In order to perform a simulation which to include the effects of such errors, the maximum possible camber of the blade profile mean line was estimated, and an altered, non-symmetric C_D/C_L performance curve has been derived.

Repeated simulations have been performed to assess the individual effects of each type of error. The blade stagger angle distortions appear to induce changes in the fluctuation component one order of magnitude larger than the non-symmetry effects. Results from a simulation for which 2 blades out of 4 had stagger angle deviations and the other two had profile mean line camber, are shown in Figure 11. Shown is only the fluctuating component of the rotor's speed for each distortion magnitude and it's spectrum. The observable effect of the blade profile deviations is a certain amplification of the fluctuations' amplitude—proportional to the magnitude of the deviation—as well as the

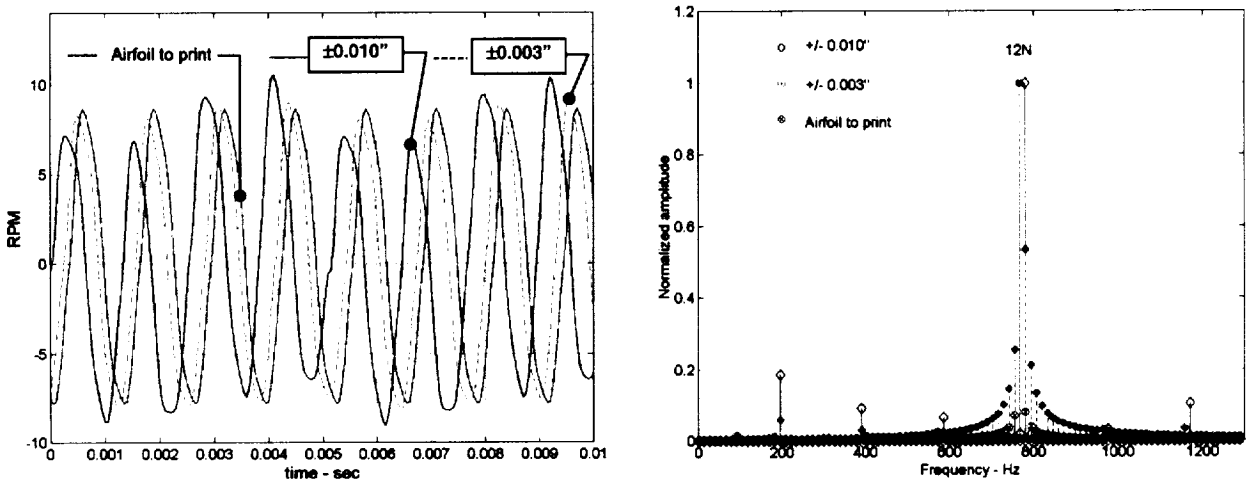

(a) *(b)*

Figure 11. Combined effects due to blade geometry distortions. Both type I and type II geometry distortions are included: two non-consecutive blades have blade stagger angle distortions of +/- max value allowed by the specified tolerance band, while the other two blades have a camber of the mean line also max and min allowed by the tolerance field. a) rotor speed fluctuating component. b) spectrum of the fluctuation. While the 12N base frequency remains unchanged, lower and upper harmonics are created.

creation of upper and lower harmonics in the fluctuation. Furthermore, a phase shift is introduced in the fluctuating speed component. This is an important effect, which will be addressed in detail in the next section. While for the ±0.003" tolerance band the fluctuation change is minimal, the distortions allowed by the ±0.010" tolerance band have a noticeable effect.

3.3 An explanation of the shifting phenomenon

The apparent shifting in the SSME flowmeter's calibration constant, Kf has been a puzzling issue for many years. Strict limitations have been imposed on the flowmeter operating parameters in order to preclude the phenomenon to occur, and all the "bad shifters" have been carefully de-selected from the fleet inventory. Many authors, mentioned in the introduction section of this study, have addressed the topic. The analysis by L. K. Sharma [3] showed analytically that the flowmeter indication is very sensitive to the incoming flow turbulence and distortions of the flow velocity field. The results of Sharma's analysis show a sensitivity to flow turbulence intensity leading to a change of 1% in the flowmeter indication for a flow turbulence intensity increase from 5% to 7%.

Here, we will show that the flowmeter's sensitivity to flow turbulence intensity couples with three other operating characteristics described in the subsections 3.1 and 3.2, and generate a change in the device's indication. Specifically the three characteristics are i)the permanent presence of a fluctuating rotor speed component, ii)the amplification of the amplitude of the fluctuation by distortions in the blade geometry, and iii) the introduction of a phase shift in the wavy fluctuation component by distortions in the blade geometry.

A simulation of the flowmeter operation at 109% Rated Power Lever has been performed for a "to print" flowmeter rotor (i.e. no geometry distortion). The results are show in figure 12. The darker curve represents the fluctuating speed component, at constant amplitude, for zero turbulence intensity. The light color curve represents the fluctuating speed component in the presence of 5% flow turbulence intensity, added into the calculation via a Monte-Carlo procedure. The flowmeter speed is measured at each blade passage by the detector, thus there are as many readings per rotation as many blades the rotor has, which is a number of four. This is somewhat equivalent to sampling of the real speed at a rate of 4 times per revolution. For the situation with zero turbulence intensity, this is shown by the square data points, which align at the same value. The perfect constant reading is due to the fact that

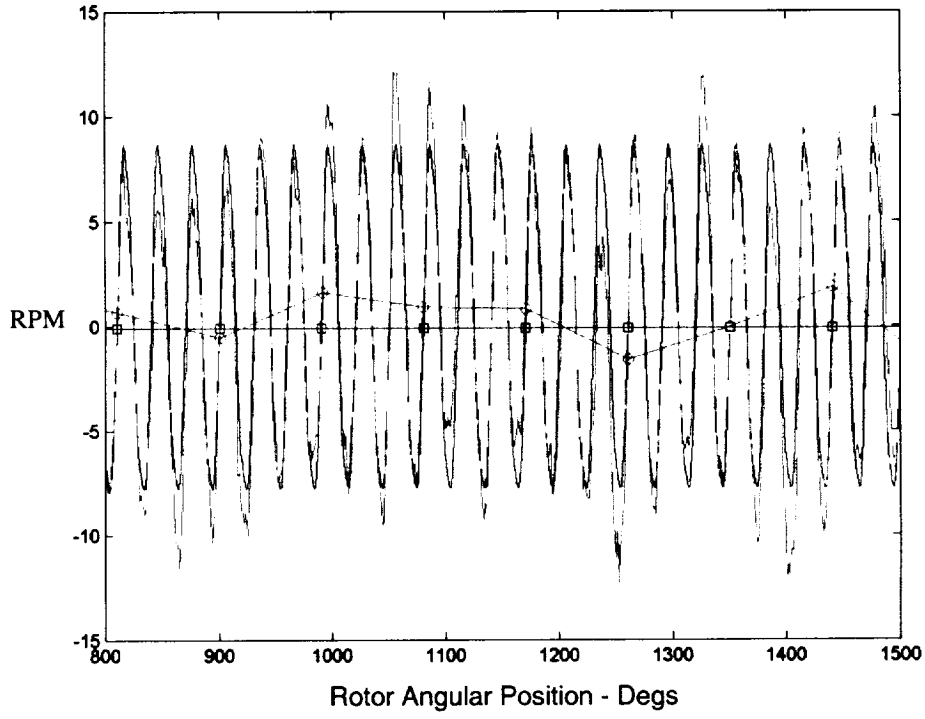

Figure 12. Speed fluctuation component for a "to print" rotor. The darker curve corresponds to zero turbulence intensity, while the light colored curve corresponds to 5% flow turbulence intensity. For each curve, the actual reading, as sampled is shown, □ - zero turbulence intensity, O- 5% turbulence intensity

the fluctuating component has a 12N periodicity, and the reading is every 4N, therefore the same value is read at every 3rd wave period. When 5 % turbulence intensity is introduced, the fluctuating speed component is perturbed in amplitude, but remains 12N periodic with no phase shift. Slight differences in the speed sampled readings reflect the amplitude perturbations, but the mean of the speed reading is essentially unchanged.

A second simulation of the flowmeter operation at 109% Rated Power Level has been performed for a distorted rotor geometry corresponding to a $+2^{o}$ and -2^{o} distortions in the blade stagger angle for two non-consecutive blades. The results are presented in Figure 13. The darker curve represents the fluctuating speed component, for zero turbulence intensity while the light color curve represents the fluctuating speed component in the presence of 5% flow turbulence intensity. The square symbols represent the speed sampling for the zero turbulence intensity. Due to the amplification and phase shift effects introduced by the distorted geometry, the sampled speed does not align at constant value, but rather fluctuates itself and introduces a small (–2.12 RPM) bias into the reading. In the presence of 5% turbulence intensity, the rotor speed fluctuations are amplified even more. The amplification is associated with a larger phase shift, which, in turn, changes the value of the sampled speed data points. This is due to the fact that the wave phase shift changed the quasi-periodical location where the wave is sampled. The mean of the sampled speed has shifted to a negative bias of –8.103 RPM, which is equivalent to an apparent shift of –0.21% in the calibration constant K_f.

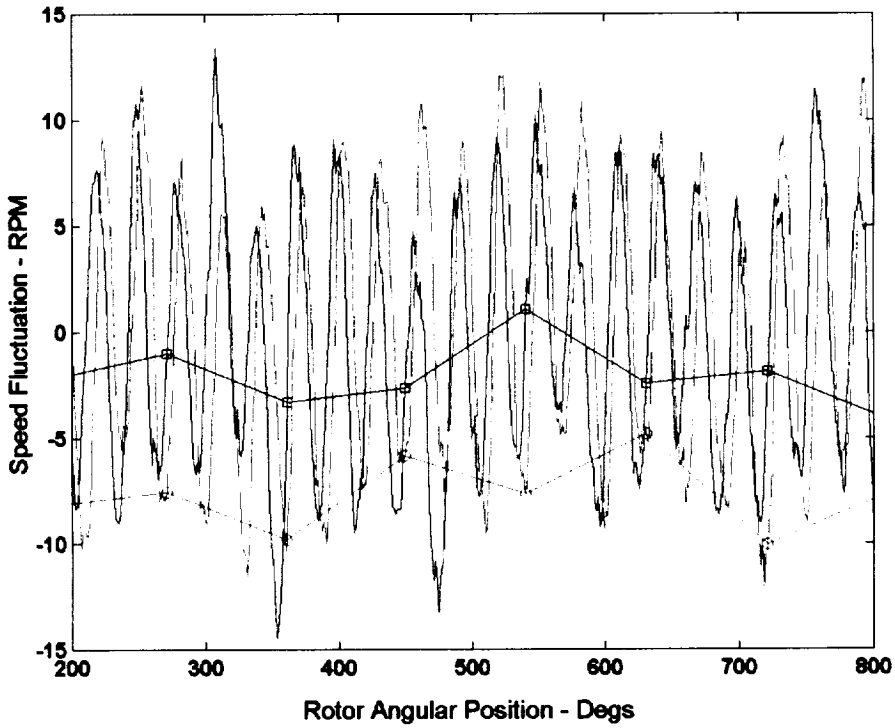

Figure 13. Speed fluctuation component for a rotor with geometry distortions due to manufacturing errors. The darker curve corresponds to zero turbulence intensity, while the light colored curve corresponds to 5% flow turbulence intensity. For each curve, the actual reading, as sampled is shown, □ - zero turbulence intensity, O- 5% turbulence intensity

The simulation presented in figure 13 explains the underlying nature of the K_f shifting phenomenon. A flowmeter with a rotor affected by distorted geometry due to manufacturing errors may shift the value of its calibration constant due to a change in the flow turbulence intensity, or due to any change in the nature of the unsteadiness characterizing the flow field behind the honeycomb flow straightener. The maximum potential value for the shifting

is roughly equivalent to the span of the rotor speed fluctuation values (max to min). The new flowmeter design [7] incorporates tight tolerances and well-studied manufacturing process to eliminate or minimize the blade geometry distortions. Furthermore, the distance from the straightener vanes to the rotors has been increased, thus allowing for a decay of the wakes in the flow field. This is equivalent to a reduction in amplitude of the rotor speed fluctuation, and thus a significant reduction in the potential value for a shift in the K_f value.

CONCLUSIONS

The present study addressed the phenomenon known as calibration constant "shifting" observed during the operation of the Space Shuttle Main Engine fuel flowmeter. The calculations are based on a synergistic model, which assembles 3-D CFD results, blade aerodynamic C_D/C_L modeling and physical dynamics of the rotor. It has been found that due to the 12N symmetry of the flow field behind the hexagonal strightener, the flowmeter rotor always operates with a rotor speed fluctuating component, which—for a "to print" rotor geometry—is stable, periodic, and of small amplitude. Distortions in the blade geometry, which alter the blade stagger angle and introduce camber to the blade airfoil mean line, are found to amplify the fluctuations in rotor speed, and introduce a phase shift. A detailed explanation as to how these effects couple with effects due to flow turbulence and generate an apparent shift in the flowmeter indications has been provided. One should note that, while the model used in the calculations reflect the physics of the phenomenon in the best possible manner, it does not capture details related to the full three-dimensionality of the flow, the effects or the rotor's presence on the flow and some details of speed sampling that were simplified for this study.

All lessons learned from the current study have been incorporated into the new SSME flowmeter design.

ACKNOWLEDGEMENTS

The author wishes to acknowledge the contributions of William Bowling-Jr for the innovative solid modeling of the rotor geometry, and error analysis for discrepant rotors. Mr. Bowling's feed back and graphic data interpretation has been extremely helpful.

Special thanks to Dr. Edward D. Lynch for providing the CFD flow field data behind the hexagonal straightener, and for the interesting discussions regarding the flow regimes and instabilities past the rotor blades.

This work was made possible through the wonderful support of the SSME management team, Mr. Gary E. Gilmartin, Mr. Henry Loureiro, and Mr. John Ubowski. Their determination towards the research and understanding of the problem addressed are fully appreciated.

REFERENCES

1. Fenwick, J.R., "Discussion of the SSME Fuel Flowmeter Anomaly", Rocketdyne Internal Report, October 13, 1993.

2. Fox. T.H., "Possible Mechanism for Flowmeter Oscillations Seen on STS-8", Mashall Space Flight Center Letter, April 9, 1984

3. L. K. Sharma, "Fuel Flowmeter Problem: Drop in Calibration Constant with Power Level", Rocketdyne Internal Report, May 13, 1988.

4. Ascoli, E. et. al. "Application of CFD to Explain Stall Behavior of the SSME Flowmeter", AIAA paper 99-2458, presented at the 35th AIAA/ASME/SAE/ASEE Joint Propulsion Conference and Exhibit.

5. Hadid, A. "Transient CFD Analysis of the SSME Fuel Flowmeter Anomaly" Rocketdyne Internal Report, May 5,1998.

6. J.T. France, "The Measurement of Fuel Flow", AGARD Flight Test Instrumentation Series, Volume 3, NATO publication, 1972.

7. Marcu, B., "Rotor Design for the SSME Fuel Flowmeter", TWAFS 1999, NASA Marshall, Huntsville, Alabama.

8. Schlichting, H. "Boundary Layer Theory", McGraw Hill, 1979

9. Abbot, I.H. and von Doenhoff, A. E.," Theory of Wing Sections", Dover , 1949.